High-speed Frictional Heating Effect on the Stress Intensity Factors of a Near-surface Line Crack

F. D. JU* and T. Y. CHEN**
*Fellow, ASME, The University of New Mexico, Albuquerque, NM USA
**Engineer, John Crane, Inc., Morton Grove, IL, USA

ABSTRACT

This paper studies the temperature field solutions and the mixed mode stress intensity factors of a half-plane medium, which contains a near-surface line crack and is excited by a moving heat source. The paper also presents and demonstrates the use of a finite difference method for the solution of the thermoelastic fracture problem. For the discrete numerical technique employed in this paper, the displacement extrapolation method is chosen for the determination of the stress intensity factors. The paper also presents effects on the stress intensity factors due to both the material properties of the medium and the location of the line crack from the wear surface.

KEYWORDS

Crack, fracture toughness (stress intensity factor), high-speed load, ligment region

INTRODUCTION

It was demonstrated that when heat flow is disturbed by the presence of defects, there is a high local intensification of temperature and its gradients in the vicinity of the defects (Anderson *et al*, 1984), causing very high thermal stresses around the defects. Such phenomenon eventually results in growth of the defects and may lead to failure. Their paper considered a near-surface cavity defect and a moving line heat source which traverses over the surface at a moderately high speed. The current paper will address the thermal phenomenon of a half-space with a near-surface line crack defect. The excitation again is a moving line heat source.

For the fracture mechanics problems, to avoid analytical complexity for complex geometries and loading conditions, numerical techniques are increasingly being used. Since the late 1960's, the finite element methods have been used for such complex fracture mechanics problems. Byskov (1970), Walsh (1970), Wilson (1971) introduced special crack tip elements, which directly modelled the square root singularity near the crack tip, combined with conventional elements covering the rest of the domain, to solve linear fracture mechanics problems. Recently, Ju and Chen (1988) extended the special elements concept to the finite difference method and successfully solved the problem of a semi-infinite body containing a rectangular cavity. The present paper, the finite difference method will be modified to solve the line crack problem.

Once a finite difference solution is obtained, the value of the stress intensity factor can be estimated by the use of the established crack tip elements. There are many practical methods which can be used to evaluate stress intensity factors. The present paper will use the displacement extrapolation method due to its relative simplicity, ease of interpretation and ready extension of the discrete data.

ANALYTICAL MODEL

The geometry of the medium will be a semi-infinite body containing a line crack. The excitation of the surface is a moving heat source as shown in Fig. 1. Since the of the line crack disrupts the homogeneity condition in the direction of traversing of the heat source, the material coordinate system which is fixed to the medium must be employed. With reference to previous work (Chen and Ju, 1988,Ju and Huanag, 1982, Ju and Liu, 1988), the analysis will use the uncoupled thermoelastic theory can be applied.

Temperature Field

The governing equation for the temperature field is the Fourier equation

$$\frac{\partial^2\phi}{\partial\xi^2} + \frac{\partial^2\phi}{\partial\eta^2} = R\,\frac{\partial\phi}{\partial\tau} \cdot \tag{1}$$

where $\phi(=Tk/q_0 d)$ is the dimensionless temperature; $(\xi,\eta)(=x_i/d)$ are the dimensionless coordinates; $\tau(=Vt/d)$ is the dimensionless time; $R(=Vd/\kappa)$ is the Peclet number; k is thermal conductivity; κ is thermal diffusivity and q_0 is the average heat flux through the contact area, and V is the traversing speed of the thermal excitation.

The temperature field ϕ satisfies the zero initial condition and the regularity condition at infinity. On the surface, heat flux is prescribed over a moving contact area. The remaining surfaces, as well as the crack surfaces, are postulated to be adiabatic.

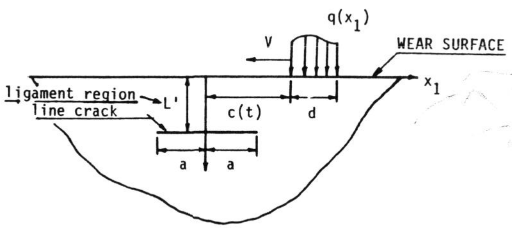

Fig. 1 Two-dimensional model

Thermal Stress Field

The thermoelastic Navier's equations and the Hooke's law are

$$N^2\frac{\partial^2 u}{\partial\xi^2} + (N^2-1)\frac{\partial^2 v}{\partial\xi\partial\eta} + \frac{\partial^2 u}{\partial\eta^2} - \frac{b^2\gamma}{c_2^{\,2}}\frac{\partial\phi}{\partial\xi} = M^2\frac{\partial^2 u}{\partial\tau^2}\,, \tag{2}$$

$$\frac{\partial^2 v}{\partial\xi^2} + (N^2-1)\frac{\partial^2 u}{\partial\xi\partial\eta} + N^2\frac{\partial^2 v}{\partial\eta^2} - \frac{b^2\gamma}{c_2^{\,2}}\frac{\partial\phi}{\partial\eta} = M^2\frac{\partial^2 v}{\partial\tau^2}\,, \tag{3}$$

$$\sigma_{\xi\xi} = N^2\frac{\partial u}{\partial\xi} + (N^2-1)\frac{\partial v}{\partial\eta} - \frac{b^2\gamma}{c_2^{\,2}}\,, \tag{4}$$

$$\sigma_{\xi\eta} = \frac{\partial u}{\partial\eta} + \frac{\partial v}{\partial\xi}\,, \tag{5}$$

and

$$\sigma_{\eta\eta} = (N^2-2)\frac{\partial u}{\partial\xi} + N^2\frac{\partial v}{\partial\eta} - \frac{b^2\gamma}{c_2^{\,2}}\,, \tag{6}$$

where $(u,v)(=u_i/d)$ are the dimensionless displacements in ξ and η direction, respectively; $(\sigma_{\xi\xi},\sigma_{\xi\eta},\sigma_{\eta\eta})(=\sigma_{ij}/\mu)$ are the dimensionless stresses; $M(=V/c_2)$ is the Mach number; $N=c_1/c_2$; $b^2=(3\lambda+2\mu)/\rho$; $\gamma=q_0 d\alpha/k$; λ and μ are Lame constants; α is thermal expansion coefficient; ρ is mass density; and c_1,c_2 are the dilatational and shear wave speed, respectively.

The medium is initially unstressed. Boundary conditions for the thermal stress field are: (i) the surface boundary and the crack surface are traction free; (ii) at infinity, the regularity conditions hold.

SOLUTION TECHNIQUE

Due to the complexity of the geometry and the boundary conditions, the finite difference method is employed to solve both the temperature field and the thermal stress field. The difference scheme will now be presented.

Temperature Field

To obtain the solution of the temperature field, an explicit finite difference scheme incorporating the energy balance method is used. The explicit finite difference scheme, the stability criteria and the energy balance method on the surface boundary are discussed in (Anderson *et al*, 1984). The procedure of the energy balance method at the crack tip is (Fig. 2)

$$Q_{W\to P} = k\,(\Delta y/2)\ \{[T^+(i-1,j,n)-t(i,j,n)]/\Delta x + [T^-(i-1,j,n)-T(i,j,n)]/\Delta x\}\,, \tag{7}$$

$$Q_{S\to P} = k\,(\Delta x)\ [T(i,j-1,n)-T(i,j,n)]/\Delta y\,, \tag{8}$$

$$Q_{Z\to P} = k\,(\Delta y)\ [T(i+1,j,n)-T(i,j,n)]/\Delta x\,, \tag{9}$$

$$Q_{N\to p} = k\,(\Delta x)\ [T(i,j+1,n)-T(i,j,n)]/\Delta y\,, \tag{10}$$

where Q is the heat flux, indexed by the flow direction, T^+ and T^- represent the temperatures of the upper and lower surfaces of the crack, respectively.

The rate of change of internal energy $\dot{U}$ in the time interval Δt at the point P(i,j) is

$$\dot{U}_P = \rho\ c\ (\Delta x \Delta y)\ [T(i,j,n+1)-T(i,j,n)]/\Delta t\ . \qquad (11)$$

Conservation of energy requires that the totality of heat flowing to the point P is equal to the rate of change of internal energy at the same point, i.e., $Q_{SUM} = \dot{U}_P$. The temperature equation at the crack tip in the dimensionless form is therefore

$$\phi(i,j,n+1) = \phi(i,j,n) + \frac{\Delta\tau}{R\Delta\xi^2}\ \{[\phi^+(i-1,j,n) + \phi^-(i-1,j,n)]/2$$

$$- 2\phi(i,j,n) + \phi(i+1,j,n)\} + \frac{\Delta\tau}{R\Delta\eta^2}\ [\phi(i,j-1,n)-2\phi(i,j,n)+$$

$$+ \phi(i,j+1,n)]\ . \qquad (12)$$

Similarly, the equations for the crack surfaces can be obtained by using the energy balance method.

Stress Field

For hard wear material such as Stellite III and a typical asperity speed, the Mach number for the thermal stress field is of the order of 10^{-3}. Since M^2 is a small parameter, the solution for the thermal stress field can be obtained by the perturbation method (Ju and Chen, 1988), using M^2 as the perturbation parameter. Since the contribution of the higher order terms may be shown to be insignificant, only the zeroth order solution is presented here.

Since high temperature and high temperature gradient are found in the vicinity of the crack, a fine mesh must be used near the line crack and a relative coarse mesh can be used in the regions away from the crack. This non-uniform mesh can be transformed parametrically to the uniform mesh and solved in the transformed plane. Discussion of the conventional finite difference equations and the coordinates transformation are referred to (Chen and Ju, 1988, Owen and Fawkes, 1983).

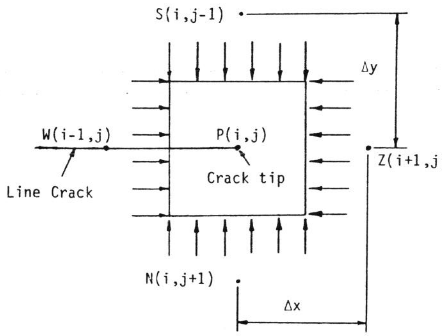

Fig. 2 Energy balance at crack tip

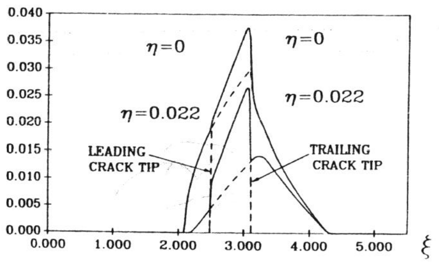

Fig. 3 Temperature distribution, L = 0.022

Special Crack Tip Elements

Since the presence of heat flow produces no additional singularities (Sih, 1962), the local character of the thermal stress singularity at the crack tip is of the same nature as that of the mechanical stress; i.e., $r^{-1/2}$. For plane thermoelastic loading conditions, the displacement field associated with the tip is described by the asymptotic equations (Walsh, 1971)

$$u = \sum_{n=1}^{\infty} \frac{r^{n/2}}{2\mu}\ \{a_n^1[(\kappa'+\frac{n}{2}+(-1)^n)\cos(\frac{n}{2})\theta - \frac{n}{2}\cos(\frac{n}{2}-2)\theta] -$$

$$- a_n^2[(\kappa'+\frac{n}{2}-(-1)^n)\sin(\frac{n}{2})\theta - \frac{n}{2}\sin(\frac{n}{2}-2)\theta]\}\ , \qquad (13)$$

and

$$v = \sum_{n=1}^{\infty} \frac{r^{n/2}}{2\mu}\ \{a_n^1[(\kappa'-\frac{n}{2}-(-1)^n)\sin(\frac{n}{2})\theta + \frac{n}{2}\sin(\frac{n}{2}-2)\theta] +$$

$$+ a_n^2[(\kappa'-\frac{n}{2}+(-1)^n)\cos(\frac{n}{2})\theta + \frac{n}{2}\cos(\frac{n}{2}-2)\theta]\}\ . \qquad (14)$$

where r is the distance measured from the crack tip, $\kappa'=3-4\nu$ for plane strain problem, ν is Poisson's ratio, a_n^1 and a_n^2 are constants to be determined. Equations (13,14) shows that the first terms of the displacement series yield stresses as a function of $r^{-1/2}$, which characterizes the stress singularity at the crack tip. In the numerical scheme, for small r, the first few terms of the displacement series dominate. The conventional finite difference equations and the special elements constitute a complete set of difference equations for finding the thermal stress field solution.

NUMERICAL RESULTS

Because of the nonsymmetrical thermal stress field associated with the mixed mode stress intensity factors are to be evaluated. Numerical computations are carried out for the following values of the parameters: V=15 m/s, a=0.3d, d=1mm. The material properties are those of Stellite III. The smallest mesh size used under the moving heat source and near the crack tips is $\Delta\xi$=0.01 and $\Delta\eta$=0.005. The mesh sizes are rapidly increased away from these two regions.

Figure 3 compares the temperature fields of the medium with and without a line crack when the heat source is directly over the crack. The ligament thickness (thickness between the wear surface and the crack surface) for the medium with a line crack is L=L'/d=0.022. In the figure, solid lines are for the medium with a line crack; and dashed lines are for the medium with no crack. The temperature field and the temperature gradient of the medium containing a line crack is much higher than those of the medium with no crack. This high temperature field and its gradients are the source of the high thermal stresses.
The plane strain displacement equations are

$$u = \frac{K_I}{4\mu}\ (r/2\pi)^{1/2}\ [(2\kappa'-1)\cos(\theta/2)-\cos(3\theta/2)]-$$

$$\frac{K_{II}}{4\mu}\ (r/2\pi)^{1/2}\ [(2\kappa'+3)\sin(\theta/2)+\sin(3\theta/2)]\ , \qquad (15)$$

and

$$v = \frac{K_I}{4\mu}(r/2\pi)^{1/2}\,[(2\kappa'+1)\sin(\theta/2)-\sin(3\theta/2)] -$$

$$\frac{K_{II}}{4\mu}(r/2\pi)^{1/2}\,[(2\kappa'+3)\cos(\theta/2)+\cos(3\theta/2)]\ , \qquad (16)$$

in which K_I and K_{II} are the mode I and the mode II stress intensity factors, and μ is the shear modulus. Substituting the values of r and u or v for nodal points along the crack surfaces emanating from the crack tip allows a plot of K_I and K_{II} against radial distance r. The approximate values of K_I and K_{II} are thus obtained by extrapolation to r=0. Fig. 4 shows the effect of the location of the moving heat source on the stress intensity factors, where $k = k/\sigma_0\sqrt{d}$ is the dimensionless stress intensity factors, d is the contact width of the moving heat source, and σ_0 = 1 unit. At the time τ=1.2, when the moving heat source is right above the line crack, both k_1 and k_2 reach a maximum value. This figure thus establishes that, when the moving heat source is right above the line crack, not only the thermal stress field but also the stress intensity factors will reach the worst state.

Figures 5-8 present the effects of the mechanical and thermal properties on the stress intensity factors when the moving heat source is right above the line crack. Figures 5 and 6 show the linear effects of the Young's modulus (E) and the coefficient of thermal expansion (α). Fig. 7 illustrates the effect of thermal conductivity (k). In this figure with fixed thermal diffusivity (κ), both k_1 and k_2 are inversely proportional to thermal conductivity, owing to the inverse relation of the thermal conductivity and result the temperature field. Fig. 8 demonstrates the effect of thermal capacity (ρc) on stress intensity factors with fixed thermal conductivity is fixed. The figure establishes that, as the thermal capacity is decreased, the mode I stress intensity factor k_1 is decreased, but the mode II stress intensity factor k_2 is increased.

The presence of defects will change the pattern of the temperature distribution. Consequently, the critical depth, at which thermal principal stress reaches a maximum, is changed. (Chen and Ju, 1988, Ju and Liu, 1988)

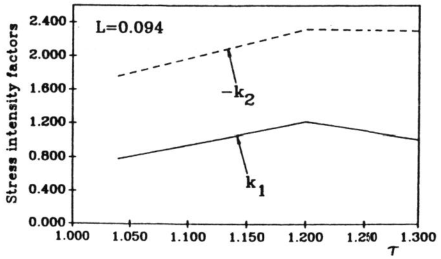

Fig. 4 Effect of the location of the moving heat source on stress intensity factors

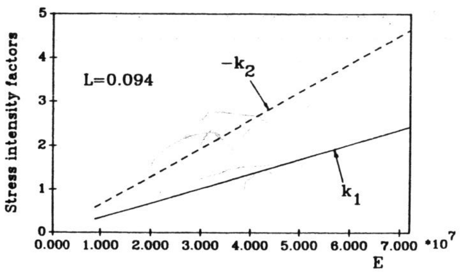

Fig. 5 Stress intensity factors vs. Young's modulus

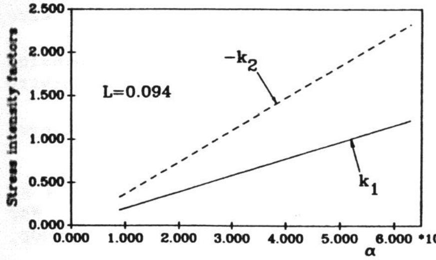

Fig. 6 Stress intensity factors vs. the coefficient of thermal expansion

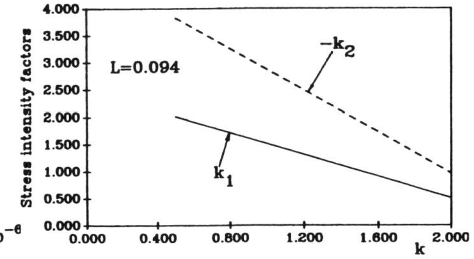

Fig. 7 Stress intensity factors vs thermal conductivity

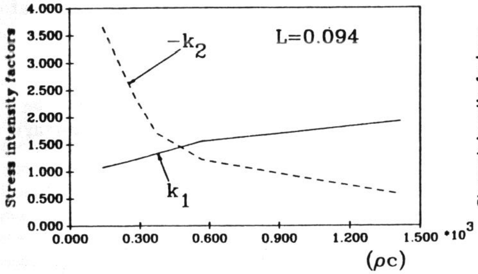

Fig. 8 Stress intensity factors vs. thermal capacity

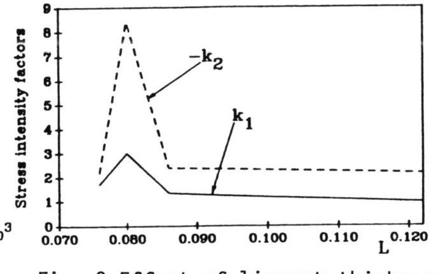

Fig. 9 Effect of ligment thickness on stress intensity factors

established that, for a medium with no defect, the critical depth, at which the principal tensile stress reaches a maximum, is η_{cr}=0.16 for Stellite III. However, when there is a rectangular cavity, the principal tensile stress is the highest at the top trailing corner of the rectangular cavity and reaches a maximum at the critical ligament thickness L_{cr}=0.094. In the present paper, it is found that the geometry of the defect will influence the critical ligament thickness. As illustrated in Fig. 9, both k_1 and k_2 reach a maximum when the ligament thickness is at L=0.08.

CONCLUSIONS

The paper demonstrates the use of the finite difference method, supplemented with a special computational procedure, to determine the stress intensity factors at the crack tip. The mixed mode stress intensity factors for a thermoelastic problem with a moving heat source excitation were considered in both the derivations and examples. The procedures developed can readily be extended to different loading conditions and different crack geometry. The perturbation method mentioned in the paper allows one to consider the various order solutions in the numerical calculations depending on the magnitude of the Mach number.

The demonstration of the numerical results, we may conclude:

(i) Because of the poor heat transfer characteristics of the crack surface, temperature and its gradients in the vicinity of a line crack are much higher than that of the medium with no defect. This high temperature and high temperature gradients are the source of large thermal stresses.

(ii) Increasing Young's modulus, the coefficient of thermal expansion and decreasing thermal conductivity will result in larger stress intensity factors, leading to earlier crack propagation.

(iii) Decreasing thermal capacity will result in smaller k_I, but larger k_{II}.

(iv) For the moving asperity problem, there is a critical depth at which the principal thermal stress reaches a maximum (Wilson, 1971). For Stellite III, the critical depth is $\eta_{cr}=0.16$, Ju and Liu, (1988). However, when there is a defect, the depth at which the maximum value of stress occurs is changed, depending on the location of the defect (Ju and Chen, 1988). For a rectangular cavity, the maximum thermal stress occurs at the ligament thickness $L_{cr}=0.094$. In this paper, we established that the geometry of the defect will also influence the critical ligament thickness. For Stellite III, the critical ligament thickness for a line crack is at $L_{cr}=0.08$.

ACKNOWLEDGMENT

The paper is part of the work performed under ONR Grant No. ONR-N00014-84-k-0252. Dr. A. William Ruff and Dr. Marshall B. Peterson are the program managers.

REFERENCES

Anderson, D.A., J.C. Tannehill, and R.H. Pletcher, (1984) Computational Fluid Mechanics and Heat Transfer, McGraw-Hill Book Company, New York.

Byskov, E., (1970), "The Calculation of Stress Intensity Factors Using the Finite Element Method with Cracked Elements," Int. J. Fracture Mech., 6, pp.159-167.

Chen, T.Y. and F.D. Ju, (1987) "Thermal Effects in a Coated Medium (with a cavity) Due to Friction Heating by a Passing Asperity," ASLE Transaction 30, 4, pp.427-435

Chen, T.Y. and F.D. Ju, (1988) "Thermomechanical Cracking in the Vicinity of a Near-Surface Void Due to High-Speed Friction Load," J. of Tribology, 110, No.2, pp. 306-312.

Huang, J.H. and F.D. Ju, (1985) "Thermomechanical Cracking Due to Moving Friction Load," part I & II, Wear, 102, pp. 81-97.

Ju, F.D. and J.H. Huang, (1982) "Heat Checking in a Contact Zone of a Bearing Seal (A Two-Dimensional Model of a Single Moving Asperity)," Wear, 79, pp. 107-118.

Ju, F.D. and J.C. Liu, (1988) "Effect of Peclet Number in Thermo-Mechanical Cracking Due to High-Speed Friction Load," J. of Tribology, 110, No.2, pp.217-221.

Owen, D.R.J. and A.J. Fawkes, (1983) Engineering Fracture Mechanics: Numerical Methods and Applications, Pineridge Press Ltd. Swansea, U.K..

Sih, G.C., (1962) "On the Singular Character of Thermal Stresses Near a Crack Tip," ASME J. of Applied Mechanics, vol. 29, Sep. pp. 587-589

Walsh, P.F., (1971) "The Computation of Stress Intensity Factors by a Special Finite Element Technique," Int. J. Solids Struct., 7, pp. 1333-1342

Wilson, W.K., (1971) "Some Crack Tip Finite Elements for Plate Elasticity in Fracture Toughness," Proc. of Fifth Nat. Symp. on Fract. Mech., ASTM STP514.